A Bio-Inspired Whisker Sensor Based on Triboelectric Nanogenerators

XINYU WANG *, PENG XU *, ZHI MA §, SIYUAN WANG *,
GUANGMING XIE †‡, MINYI XU *†
*Marine Engineering College, Dalian Maritime University, Dalian 116026, China
†The State Key Laboratory of Turbulence and Complex Systems, Intelligent Biomimetic Design Lab,
College of Engineering, Peking University, Beijing,100871, China
‡Peng Cheng Laboratory, Shenzhen 518000, China
§Navigation College, Dalian Maritime University, Dalian 116026, China

2020 35th Youth Academic Annual Conference of Chinese Association of Automation (YAC) | 978-1-7281-7684-0/20/$31.00 ©2020 IEEE | DOI: 10.1109/YAC51587.2020.9337588

***Abstract*—Perceptual sensors play a crucial role in the next generation of robots due to their potential application in agriculture, biomedicine and industry fields. In this field, with dependence on visual, auditory and tactile techniques, sensors are utilized to intelligently assess their environment. Here, this study investigates a bio-inspired whisker sensor with self-power capability based on triboelectric nanogenerators (TENG) for building an robotic perceptual system. The whisker sensor is composed of cylindrical structure house (52mm in height and 10mm in diameter), a PTFE pellet fixed to the spring-fixed base, four copper (Cu) films attached symmetrically to inner of house, and memory alloys (50mm in length). Generally, the displacement of the whisker rod causes the change in voltage in four direction because of generated tensile. From experiments to data analysis and modeling, the sensor is characterized by simple structure, convenient fabrication, high sensitivity and self power supply without external power supply. Thus, this 3D printable self-powered whisker sensor should be applicable to a wide range of automaton applications.**

***Keywords*—Self-powered; Whisker Sensor; Triboelectric Nanogenerator; Perceptual System**

I. Introduction

The rapid development of robotic technology has liberated labor, but also bring several grand challenges related to the robots industry in the next generation [1]. As the most efficient and straightforward perceptual strategy, one standard for robots' perceptual systems requires the robots to intelligently assess their environment for fulfilling complex tasks. Traditionally, robots' perceptual systems typically rely on visual and auditory techniques. However, robots are not able to work properly without the cues of visual and auditory. To facilitate widespread applications in robots, the perceptual sensor in a robot system should mimic animal with their whiskers to identify the positions of objects, particularly in dark surroundings. In the existing work [2], [3], models of whisker follicles including both the follicle mechanical and nerve structures is proposed, which leads to complex higher order dynamics. On the basis of follicle structure, piezoelectric material or hall element is utilized to design whisker for modelling the environment [4], distinguishing two lookalike textures with assistant of variations of stiffness [5], measuring both contact and fluid motion [6].

On the other hand, most robots are space-constrained with limited inner volume, as well as highly limited payload energy, and therefore typically require designed sensors characterized by light-weight, small-size, inexpensive to manufacture and low-powered. Besides, developing new energy-storing material and technology can promote the developments in robots' perceptual systems using a whisker-inspired sensor with high sensitivity. Motivated by the aforementioned, a triboelectric nanogenerator (TENG) coupled with triboelectrification and electrostatic induction has been developed as a new electromechanical conversion technology, which exhibits diverse applications in both energy harvesting and self-powered mechanical sensing [7], [8]. Based on its unique working mechanism, self-powered triboelectric sensors have shown responding to the stimulation from the environment without further energy supply devices [9], ultrahigh sensitivity to the vocal intonations [10], measuring the vibration of mechanical equipment and human motion in real time [11]. By taking advantage of various materials and simple structures, [12] demonstrated a triboelectric highly-sensitive wave device based on liquid-solid interfacing. Furthermore, Developing skin-like sensory devices allows them to naturally sense and interact with environment [13]. With these capabilities, a triboelectric whisker-inspired sensor (TWS) could provide a simple scheme to the motion perception.

Here, we describe a easy-fabrication, contact-separation channel, and self-powered TWS for constructing robots' perceptual system. Fig.3(b) presents a structure based on rats' follicle models is the more important dynamics that can affect whisker sensing. For measuring simplicity, the data are obtained separately by bending the whisker in four directions, that is, up, down, left, and right and compared afterward. Specifically, the whisker rod section protrudes from a housing section. A 3D model of the whisker sensors is shown in Fig.3(c), where a poly tetra fluoroethylene (PTFE) pellet fixed to the spring-fixed base is connected to the root of a memory metal shaft. Four copper (Cu) electrodes are rigidly mounted at inner surface of house.

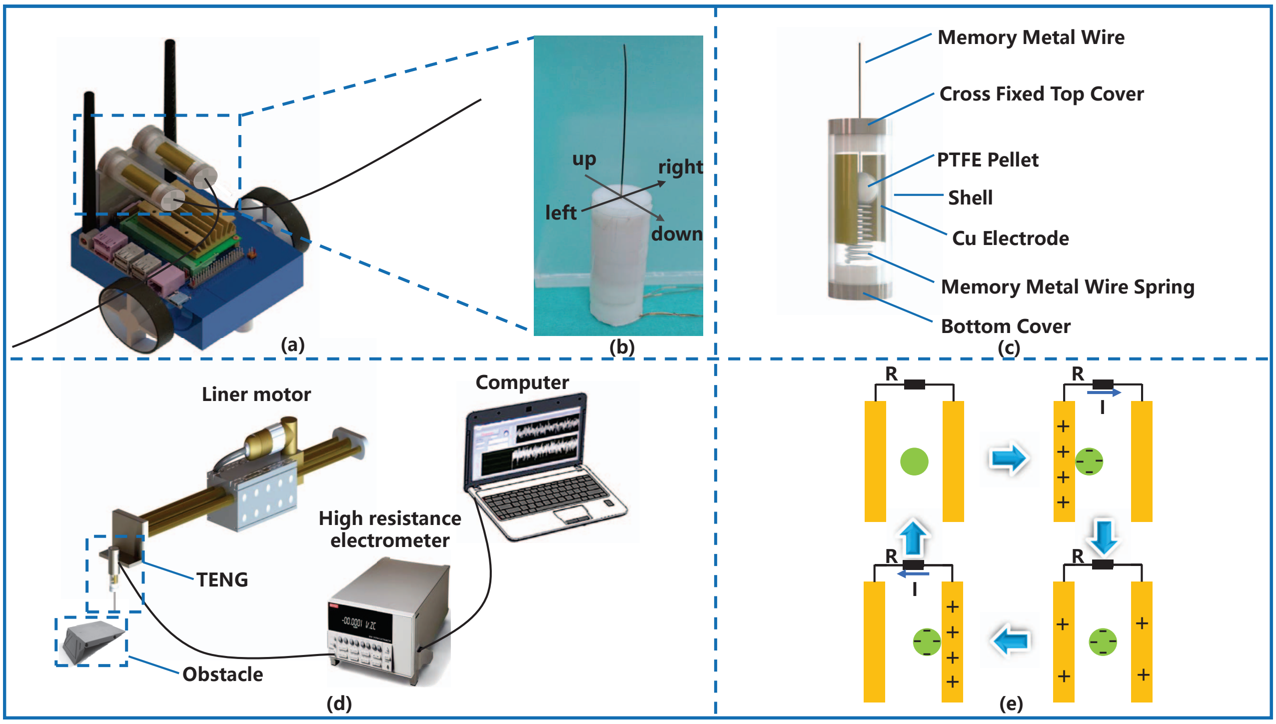

Fig. 1. Application, structure and working mechanism of bionic follicle whisker sensor. (a) Application of bionic follicle whisker sensor. (b) Physical picture of bionic follicle whisker sensor. (c) Structure scheme of bionic follicle whisker. (d) Platform of experiment. (e) Working mechanism of the bionic follicle whisker sensor.

II. Design

Inspired by the follicle structure of rats' whisker, Fig.1 introduces the application, structure and working mechanism of the triboelectric whisker-inspired sensor. Fig.1(a) indicates the two TWS are placed on the front the automaton. When the automaton touches an obstacle, it receives the acknowledgement of this fact from its sensors. The physical model of the TWS presents that the whisker rod section protrudes from a housing section, as shown in Fig.1(b). Evidently, the data are obtained separately by bending the whisker in four directions, that is, up, down, left, and right and compared afterward. Fig.1(c) describes the structure of the TWS. A housing section of the TWS adopts a cylindrical structure (52mm in height and 10mm in diameter) produced by 3D printing in PLA (polylactic acid, a kind of materials in 3D printing). The Cu films (30mm in length and 10mm in width) are rigidly mounted at inner surface of house in four directions. The whisker rod section adopts a thin rod made of shape memory alloys (SMA) (50mm in length). Then, the PTFE pellet fixed to the spring-fixed base is connected to the root of the whisker shaft, and its starting position is in contact with each of the Cu electrode. The displacement of the PTFE pellet driven by any small deflection of whisker shaft can produce a change in voltage signal. The sequence is thus: deflection of the whisker rod drives the PTFE pellet to touch on the Cu electrodes, which produce voltage output and thereby provide deflection information.

The TWS is characterized in s series of experiments performed using linear motors. Fig.1(d) shows the experiments setup. At different frequencies and amplitudes, linear motors drives the TWS to touch the obstacles initiatively. The electron signal produced by the TWS is measured by a Keithley 6514 electrometer. And the signal shows clearly on Labview software of the computer after the acceptance of electrometer.

Fig.1(e) illustrates the working mechanism of the TWS. The impact between the whisker and obstacle, causing the PTFE pellet to oscillate repeatedly. When the PTFE pellet is in contact with the Cu film on the left side, the electron clouds on the surfaces of two materials overlap and some of the electrons from the copper film enter the deeper potential well of PTFE pellet. Owing to the higher electronegativity of PTFE than copper, the surface of PTFE pellet becomes negatively charged and the Cu film becomes positively charged. Due to the movement of the PTFE pellet, the pellet separates from the Cu film. As the positive and negative triboelectric charges are not coincide on the same plane which generates electrical potential between the PTFE pellet and Cu film. Therefore, free electrons transfer from the PTFE pellet to the Cu film to balance the electric field. The transfer of free electrons stop until the separation of the PTFE pellet and Cu film is maximized. Then the PTFE pellet move continuously towards to Cu film on the right side which cause another electric potential and the free electrons flow. Thereafter, the PTFE pellet move back to the neutral position. Finally, the distribute of electric charge return to its initial state and a cycle of electricity signal generation has been completed.

III. Experiments and Results

The working mechanism of the TWS is further verified using COMSOL software, as shown Fig.2(a), where the results of the potential distribution is given between the PTFE pellet and Cu film in the different position. The TWS has four displacement directions under the restriction of the "cross-shaped" opening, such as, up, down, left and right. During the experiment, a linear motor is used to drive the TWS to touch obstacles.

Subsequently, under condition $f = 0.3Hz$, Fig.2(b) shows the influences of the displacement in the up direction on the output performance of the TWS. As the displacement gradually increasing from $0.5cm$ to $10cm$, the peak values of output voltage all first increase and then attain a plateau value, which may caused by the limitation of material and the size of material.

Fig.2(c) illustrates the output performance of the TWS under the condition $f = 0.1 - 1Hz$ and $d = 5cm$ in the up direction. Evidently, the output voltage of the sensor is almost constant when the frequency increase from $0.1Hz$ to $1Hz$. It is interesting to find that frequency has little effect on the output voltage of the TWS.

Fig.2(d)- (e) describes the influences of the displacement in the left and down direction on the output performance of the TWS. Similarly, it varies in the frequency of $0.3Hz$ and its peak value increases from 0.26 to $0.92V$ by increasing displacement from $0.5cm$ to $10cm$. Note that different from the output performance in Fig.2(c) and Fig.2(d), the falling edge is generated at the peak values of output voltage in Fig.2(e). Based on this characteristics, a direction of the deflection information may be attained from the output voltage. Furthermore, size and shape of the obstacle can be determined by the array of the TWS.

IV. Characterization

The voltage output of TWS is related to the tip displacement of the whisker. Fig.3 shows the voltage signal of the TWS over the incremental tip displacement in four direction, where d denotes PTFE pellet displacement(mm). It confirms that the sensor model performs well at all displacement, and corresponding equations are given below.

$$V_1 = -0.005265d_1^2 + 0.09621d_1 + 0.366$$
$$V_2 = -0.006146d_2^2 + 0.1303d_2 + 0.2359$$
$$V_3 = 0.04005d_3 + 0.7284$$
$$V_4 = -0.006048d_4^2 + 0.1265d_4 + 0.3525$$

where the corresponding R2 values, the coefficient of determination, are 0.9889, 0.9907, 0.9875, and 0.9537 in sequential order.

It is interesting results that sensor in Left direction can be curved as a linear relationship between voltage and PTFE pellet displacement But sensor in Up, Down and Right direction are best characterized by a quadratic one. These characterization equations can provide a guideline for engineering application.

V. Conclusion

A kind of bionic follicle whisker sensor based on the principle of triboelectric nanogenerators is designed. The sensor has the characteristics of simple structure, convenient fabrication, high sensitivity and self power supply without external power supply. The structure of the sensor is designed to be similar to the whisker. The inner shell of the follicle is equipped with a touch sensing device. When an external object collides with the whisker, the whisker deviates from the middle position and then causes the mutual distance between the electrodes. The signal can be generated by electrostatic induction. Through the experimental research and analysis, the experimental data processing reveals the law of sensor induction and establishes the data analysis model, which lays the foundation for further research in the future.

Acknowledgment

This work was supported by National Natural Science Foundation of China (Grant No. 51879022, 91648120, 61633002, 51575005, 61503008). Peng Xu and Mingyi Xu are Corresponding authors.

References

[1] G.-Z. Yang, J. Bellingham, P. E. Dupont, P. Fischer, L. Floridi, R. Full, N. Jacobstein, V. Kumar, M. McNutt, R. Merrifield *et al.*, "The grand challenges of science robotics," *Science Robotics*, vol. 3, no. 14, p. eaar7650, 2018.

[2] B. Mitchinson, E. Arabzadeh, M. E. Diamond, and T. J. Prescott, "Spike-timing in primary sensory neurons: a model of somatosensory transduction in the rat," *Biological cybernetics*, vol. 98, no. 3, pp. 185–194, 2008.

[3] B. Mitchinson, K. N. Gurney, P. Redgrave, C. Melhuish, A. G. Pipe, M. Pearson, I. Gilhespy, and T. J. Prescott, "Empirically inspired simulated electro-mechanical model of the rat mystacial follicle-sinus complex," *Proceedings of the Royal Society of London. Series B: Biological Sciences*, vol. 271, no. 1556, pp. 2509–2516, 2004.

[4] T. J. Prescott, M. J. Pearson, B. Mitchinson, J. C. W. Sullivan, and A. G. Pipe, "Whisking with robots," *IEEE robotics & automation magazine*, vol. 16, no. 3, pp. 42–50, 2009.

[5] H. Wegiriya, N. Herzig, S.-A. Abad, S. H. Sadati, and T. Nanayakkara, "A stiffness controllable multimodal whisker sensor follicle for texture comparison," *IEEE Sensors Journal*, 2019.

[6] W. Deer and P. E. Pounds, "Lightweight whiskers for contact, pre-contact, and fluid velocity sensing," *IEEE Robotics and Automation Letters*, vol. 4, no. 2, pp. 1978–1984, 2019.

[7] F.-R. Fan, Z.-Q. Tian, and Z. L. Wang, "Flexible triboelectric generator," *Nano energy*, vol. 1, no. 2, pp. 328–334, 2012.

[8] Z. L. Wang, T. Jiang, and L. Xu, "Toward the blue energy dream by triboelectric nanogenerator networks," *Nano Energy*, vol. 39, pp. 9–23, 2017.

[9] H. Chen, Y. Song, X. Cheng, and H. Zhang, "Self-powered electronic skin based on the triboelectric generator," *Nano energy*, vol. 56, pp. 252–268, 2019.

[10] H. Guo, X. Pu, J. Chen, Y. Meng, M.-H. Yeh, G. Liu, Q. Tang, B. Chen, D. Liu, S. Qi *et al.*, "A highly sensitive, self-powered triboelectric auditory sensor for social robotics and hearing aids," *Science Robotics*, vol. 3, no. 20, p. eaat2516, 2018.

[11] B. Zhang, L. Zhang, W. Deng, L. Jin, F. Chun, H. Pan, B. Gu, H. Zhang, Z. Lv, W. Yang *et al.*, "Self-powered acceleration sensor based on liquid metal triboelectric nanogenerator for vibration monitoring," *ACS nano*, vol. 11, no. 7, pp. 7440–7446, 2017.

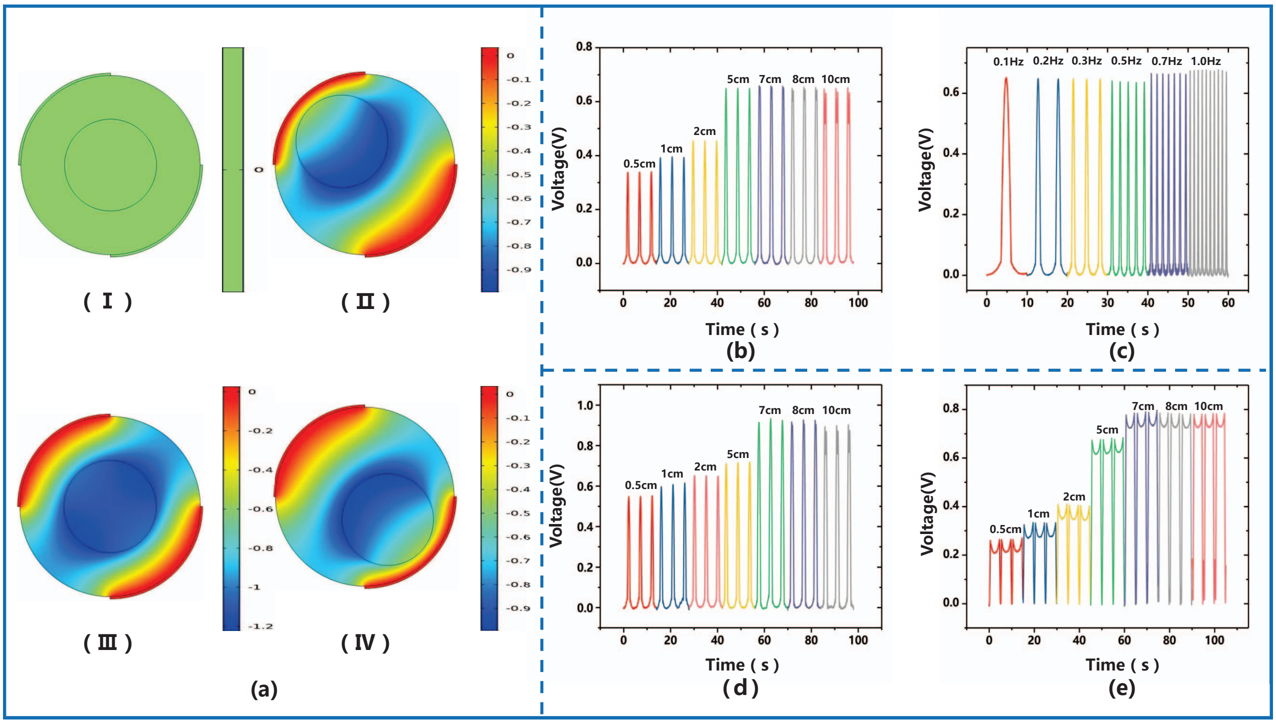

Fig. 2. (a) the simulation of the potential distribution between the PTFE pellet and Cu film in the different position obtained by COMSOL software (b) the output performance of the whisker sensor in the up direction at different amplitudes of the linear motor (c) the output performance of the whisker sensor in the up direction at different frequency of the linear motor (d) the voltage signal obtained when the whisker sensor in the left direction (e) the signal output by the whisker sensor at different amplitudes of the linear motor in the down direction.

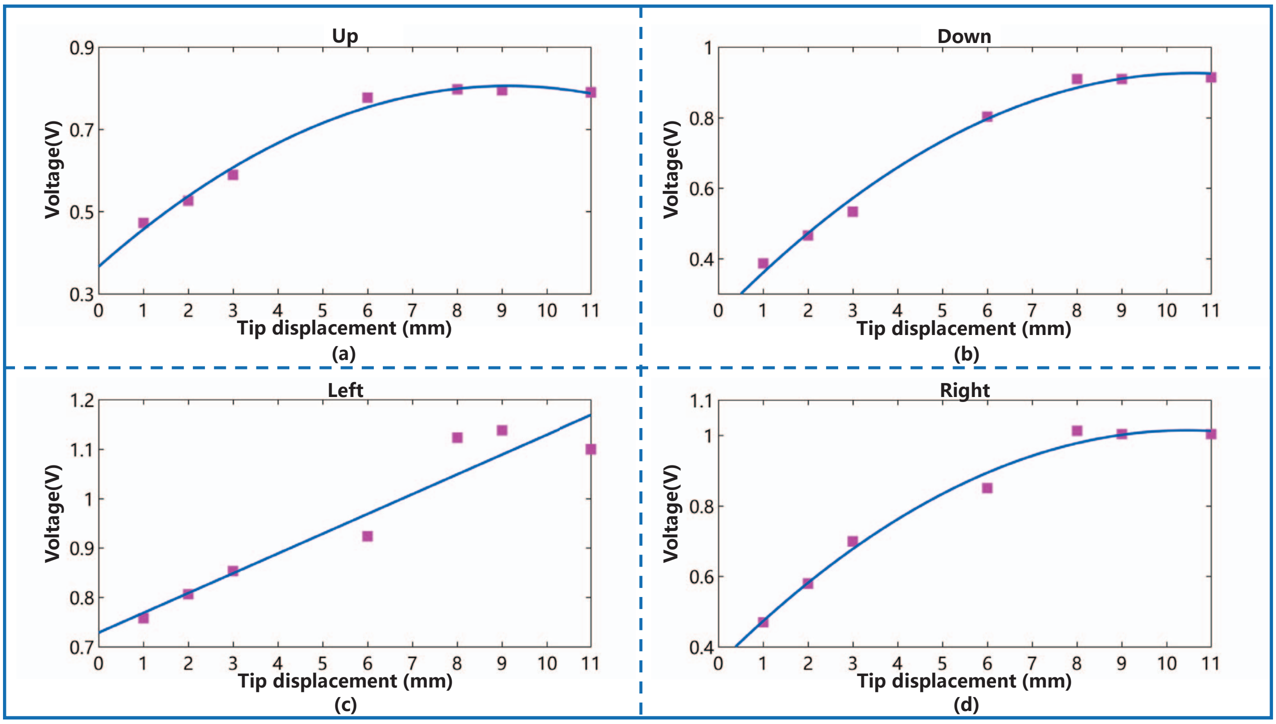

Fig. 3. Voltage output for four directions of whisker sensor over the incremental tip displacement.

[12] M. Xu, S. Wang, S. L. Zhang, W. Ding, P. T. Kien, C. Wang, Z. Li, X. Pan, and Z. L. Wang, "A highly-sensitive wave sensor based on liquid-solid interfacing triboelectric nanogenerator for smart marine equipment," *Nano Energy*, vol. 57, pp. 574–580, 2019.

[13] Y.-C. Lai, J. Deng, R. Liu, Y.-C. Hsiao, S. L. Zhang, W. Peng, H.-M. Wu, X. Wang, and Z. L. Wang, "Actively perceiving and responsive soft robots enabled by self-powered, highly extensible, and highly sensitive triboelectric proximity-and pressure-sensing skins," *Advanced Materials*, vol. 30, no. 28, p. 1801114, 2018.